Numerical Study of Fluid Dynamics and Heat Transfer in a PEM Fuel Cell Stack

J. M. Sierra[1,*], S. J. Figueroa-Ramírez[1], C. Patiño-Carachure[1], S. Díaz[1], O. Meza[1], M. A. Meza[1]

[1] Facultad de Ingeniería, Universidad Autónoma del Carmen, Cd. del Carmen, Campeche, México, 24115.
[*]Tel: +52(777)1843585; e-mail: juanmsg@live.com.mx

ABSTRACT

In this work, a numerical study of fluid dynamics and heat transfer in the flow distributor of a PEM fuel cell is presented. The aim of this work is focused on studying the pressure drops and temperature variations presented by stacks with serpentine channels. Different fuel cells with flow fields of 1, 2 and 3 parallel channels; active areas of 5 and 25 cm^2; and stacks with 3 and 5 assemblies were evaluated. From simulation results, it was found that the use of channels in parallel improves the gas distribution inside the fuel cell, increasing of this way the utilization of fuel and oxidant. Also, it was observed that the relationship between the channel width and the active area of the fuel cell is considered as an important factor in the design of the flow field. If this relationship is not taken into account, the pressure drops that occur in the flow channels will impact the overall performance of the stack. Moreover, based on the heat transfer study were identified the spots with more temperature variation in fuel cell and it could be demonstrated that heat convection is the mechanism by which the fuel cell dissipates its heat.

*Keywords:*Flow field; Stack; CFD.

1. Introduction

One of the most promising technologies at the new hydrogen economy are the fuel cells. These are characterized by their high conversion efficiency, modularity and zero pollution. Their advantages have made them a leading technology that can replace the internal combustion engines in transportation and batteries in portable applications [1]. Currently there are different types of fuel cells, which are distinguished by the operating temperature and the electrolyte. However, the proton exchange membrane (PEM) fuel cell has gained more attention by their low operating temperature and high efficiency. The operation of a fuel cell is simple, hydrogen and oxygen are supplied separately to the cell and they react electrochemically to generate electricity, the only products obtained are water and heat. The reactions that take place at the anode and the cathode of the fuel cell are described below:

$$2H_2 \rightarrow 4H^+ + 4e^- \quad (1)$$

$$O_2 + 4H^+ + 4e^- \rightarrow 2H_2O \quad (2)$$

A fuel cell is composed of a membrane, catalyst layers, gas diffusion layers and bipolar plates. The membrane (electrolyte) is a perfluorosulfonic acid commonly called Nafion, which allows the transport of H^+ ions from the anode to the cathode, next there are the catalyst layers or electrodes (anode and cathode), the zones were oxidation and reduction reactions take place. The catalyst layers are composed essentially of Vulcan carbon and platinum particles. The electrodes and electrolyte together form the membrane-electrode assembly (MEA), the main component of the fuel cell. Next to the catalyst layers are the gas diffusion layers, which are made of carbon paper or carbon cloth, these are porous zones that allow the uniform distribution of reactant gases over the catalyst layers. Finally, there are the bipolar plates, which are made from graphite and give mechanical support and electrical contact to the fuel cell besides containing channels that supply the reactant gases into the electrochemical device.

In spite of the PEM fuel cell operation can be described in a simple form, its performance is considerably affected by the operating conditions of pressure, temperature and gas composition, as well as the material properties that compose it. These factors influence considerably on the cell potential, the magnitude of the activation overpotential, the ohmic resistance and the mass transport losses that characterize the fuel cell [2].

In recent years there have been many efforts to minimize these losses, through the development of new catalytic materials and different types of novel electrolytes [3, 4]; however few studies have been reported on the flow field designs and the bipolar plates [5]. It is important to take into account that the performance of a stack depends on the sum of the performance of all its components and this correlation has not been achieved in a practical way so far. One of the main troubles that arise in the stack is the poor distribution of reactant gases into the cell, which is reflected in a non-uniform distribution of current density, dead zones in the membrane, hot spots, degradation of the membrane-electrode assembly and in general a poor performance of the cell [6]. Although this issue has been given enough attention by using numerical simulation and experimental analysis, there are still too many design alternatives to improve the fuel cell performance.

Recent reports about flow field designs indicate that each channel configuration has advantages and disadvantages, which depend on the operating conditions for which they were designed. The most common designs are classified into serpentine, straight channels, interdigitated, columns, mesh, and cascade designs [6, 7].

The flow field with the simplest configuration is the straight channel version, this design works efficiently and causes low pressure drops although requires ideal conditions for good performance, for example, when the flows are not supplied with enough pressure a non-uniform distribution of gases on the catalyst layer is developed. Likewise, any water droplet formed in the flow field blocks the channels. Probably, the most common design used in commercial fuel cells is the serpentine flow field, either with single or multiple channels. In this design the gas flows through the channels circulating throughout the active area of the fuel cell. This configuration increases both, the flow speed and the pressure drop; furthermore it improves the water and heat management by transporting liquid and vapor water through the channels [6, 7]. The interdigitated flow field was designed on a dead-end channel concept, which forces the gases to flow through the gas diffusion layers before they leave the plate. This structure induces forced water removal from the open structure of the gas diffusion layer but it also induces higher pressure drops between the inlet and the outlet than those of the through-flow options [5].Their advantages and drawbacks were reported in other works. [8, 9].

Although in the literature have been reported several studies of CFD in the flow fields, most of them are focused on single cell and are very few studies aimed at stacks. In this regard, the aim of this work is focused on studying the pressure drops and temperature variations presented by stacks with serpentine channels. Different fuel cells with flow fields of 1, 2 and 3 parallel channels; active areas of 5 and 25 cm^2; and stacks with 3 and 5 assemblies are evaluated in this work.

2. Description of the computational model

The computational models evaluated in this work consist of two types of fuel cells: (1) Conventional fuel cells with 5 and 25 cm^2 of active area (Fig. 1), that include gas diffusion layers (GDL), catalyst layers (CL), membrane (MEM) and monopolar plates (MP), and (2) Half-cells in stack with 5 and 25 cm^2 of active area (Fig. 2), that include a gas diffusion layer (GDL), a porous media (PM), and cathode plate (CP). The cathode compartment was simulated as stack because the oxygen reduction reaction has the lowest performance in the fuel cell. The dimensions of the components are specified in Table 1.

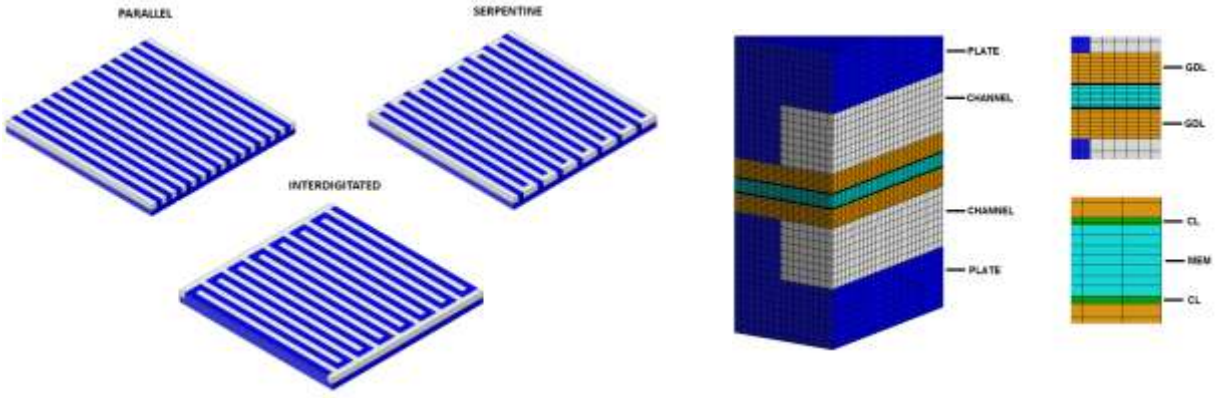

Fig. 1. Computational models of single fuel cells with 5 cm^2 of active area, conventional flow-fields (left), mesh visualization and components (right).

In order to establish the accuracy of the results and to ensure that they were independent of the grid, previous simulations were performed. The reference parameter used to do the analysis in stacks was the average pressure, and

for single fuel cells was the average current density. The final mesh used in the models had the following intervals: channels and plates (0.1), GDL's (0035), MEM (0025), and CL's (0004). The mesh elements obtained in the stacks with only one assembly was around 7.8 million and for single fuel cells was 3.5 million.

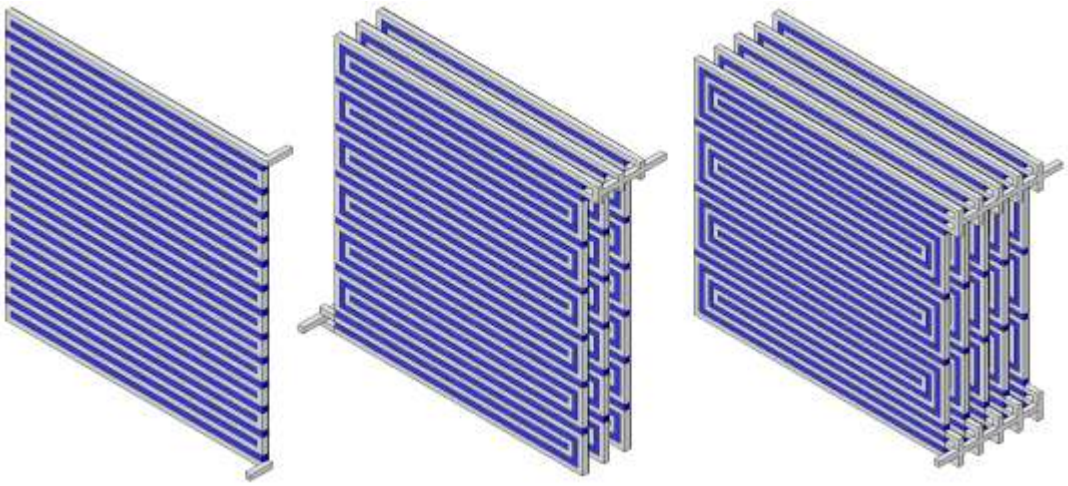

Fig. 2. Stacks of 25 cm^2 of active area, (a) single serpentine of 1 assembly, (b) double serpentine of 3 assemblies, and (c) triple serpentine of 5 assemblies.

The assumptions to carry out the numerical simulation of the computational models were the following: (a) steady state conditions, (b) laminar flow in channels, (c) isotropic porous zones, (d) the electrochemical reactions take place on the catalyst layer surface, (e) transport of species in the gas phase, and (f) the transport of liquid water in the membrane is controlled by diffusion mechanisms and electro-osmotic drag.

Table 1. Dimensions of the PEM fuel cell components.

	unit	value
Channel width	mm	0.8
Channel height	mm	0.8
Plate thickness	mm	1.6
Active area	mm^2	549
GDL thickness	mm	0.25
CL thickness	mm	0.02
MEM thickness	mm	0.178

2.1 Mathematical Model

Transport phenomena occurring inside a PEM fuel cell are represented by the governing equations of mass conservation, momentum, energy, species and charge transport. These equations are described below.

2.1.1 Continuity equation

The continuity equation represents the mass conservation for all transport processes that take place in the fuel cell, such as fluid flow, mass diffusion, phase change and electrochemical reactions. This equation is written in a simplified form (steady state) as:

$$\nabla \cdot (\rho \vec{v}) = S_m \tag{3}$$

where ρ is the fluid density, $\vec{\boldsymbol{v}}$ is the vector velocity and S_m is the source term for the species balance.

2.1.2 Momentum transport

The momentum transport equation in a steady state is described by:

$$\boldsymbol{\nabla \cdot (\rho \vec{v} \vec{v}) = -\nabla p + \nabla \cdot \left(\mu^{eff} \nabla \vec{v}\right) + S_p} \tag{4}$$

where p is the static pressure, μ^{eff} is the average viscosity of the mixture and S_p is a source term that contains the physical characteristics of porous media and it is defined as:

$$\boldsymbol{S_p = -(\mu/k)\vec{v}} \tag{5}$$

where μ is the gas viscosity (kg/m·s), k is the permeability (gas diffusion layers and catalyst layers), and $\vec{\boldsymbol{v}}$ is the superficial vector velocity at the porous media (m/s) [11].

2.1.3 Species transport

The species transport equation represents the mass conservation for each individual species of a gas. To determine the local mass fraction of each species y_i, the following equation is used:

$$\boldsymbol{\nabla \cdot (\rho \vec{v} y_i) = -\nabla \cdot \vec{J}_i + S_i} \tag{6}$$

where S_i is the source term for each phase, $\vec{\boldsymbol{J}}_{\boldsymbol{i}}$ is the flux diffusion for the species i, which is calculated for a laminar flow as:

$$\boldsymbol{\vec{J}_i = -\rho D_i \nabla \cdot y_i} \tag{7}$$

where D_i is the diffusion coefficient for the species i.

2.1.4 Energy

The energy equation for steady state is expressed by:

$$\nabla \cdot [\vec{v}(\rho E + p)] = \nabla \cdot \left(k_{eff} \nabla T - \sum_i h_i \vec{J}_i\right) \quad (8)$$

where E is the total energy, k_{eff} is the effective conductivity and $\vec{J}_i$ is the flux diffusion for the species i.

2.1.5 Electrochemical model

The fluid dynamics equations preceding this section were coupled to the electrochemical model using a commercial fuel cell module implemented in Ansys-Fluent®. This set of equations allows to solve the transport phenomena and electrochemical processes occurring in the fuel cell. This model consists of two equations for solving the two potential fields: equation (9) associated with the transport of electrons in the catalyst layers, the gas diffusion layers and the plates and, equation (10) associated to proton transport through the membrane and the catalyst layers.

$$\nabla \cdot (\sigma_{sol} \nabla \varphi_{sol}) + R_{sol} = 0 \quad (9)$$

$$\nabla \cdot (\sigma_{mem} \nabla \varphi_{mem}) + R_{mem} = 0 \quad (10)$$

where σ is the electric or ionic conductivity, φ is the cell potential and R is the transfer current; the subscripts *sol* and *mem* correspond to the solid and the electrolyte phases, respectively.

The transfer current or source terms in equations 9 and 10 are determined from the general Butler-Volmer formulation, which is used to calculate the local current density on the catalyst layers by the following equations:

$$R_{an} = j_{an}^{ref} \left(H_2 / H_{2,ref}\right)^{\gamma_{an}} \left(e^{\alpha_{an} F \eta_{an}/RT} - e^{\alpha_{ca} F \eta_{an}/RT}\right) \quad (11)$$

$$R_{ca} = j_{ca}^{ref} \left(O_2 / O_{2,ref}\right)^{\gamma_{ca}} \left(-e^{\alpha_{an} F \eta_{ca}/RT} + e^{-\alpha_{ca} F \eta_{ca}/RT}\right) \quad (12)$$

where j^{ref} is the exchange current density, H_2 y $H_{2,ref}$, are the local and reference species concentrations, γ is the concentration coefficient, α is the transfer coefficient, η is the activation losses defined in equations 13 and 14, and F is the Faraday constant (9.65×10^7 C. kg^{-1} mol^{-1}).

The reaction kinetics is controlled by the local surface overpotential, η, known as activation losses, which is associated with the difference of surface potentials between the electrode and the electrolyte φ_{sol} and φ_{mem}. This overpotential is calculated for both the anode and the cathode, including as last term the open circuit voltage (V_{OC}) and thus establishing the potential difference between both electrodes.

$$\eta_{an} = \varphi_{sol} - \varphi_{mem} \quad (13)$$

$$\eta_{ca} = \varphi_{sol} - \varphi_{mem} - V_{oc} \quad (14)$$

The membrane is modeled as a porous zone and its properties such as ionic conductivity σ_{mem} and the electro-osmotic drag coefficient are evaluated as a function of the water content λ. These properties are represented by the correlations reported by T. E. Springer et. al [12] (equations 15-17):

$$\sigma_{mem} = (0.00514\lambda - 0.00326)e^{1268\left(\frac{1}{303}-\frac{1}{T}\right)} \quad (15)$$

$$\lambda = 0.043 + 17.81a - 39.84a^2 + 36a^3 (a < 1) \quad (16)$$

where *a* is the water activity. The saturation model reported by T. Nguyen [13] and J. H. Nam et. al. [14] is used to model the formation and transport of liquid water in the membrane-electrode assembly. From these equations (9-16) both potential fields are solved, also the electrochemical process that causes the three potential losses in a fuel cell are included, which are known as: activation overpotential, ohmic overpotential and concentration overpotential.The operating conditions and the electrochemical parameters used in the simulation were taken from experimental data and literature data [15-18].

2.1.6 Boundary conditions

The boundary conditions applied to the computational domain of single fuel cell were (1) mass flow inlet, (2) pressure outlet, (3) constant potential at anode and, (4) variable potential at cathode, which were set to calculate the current density in the cell. The flows of hydrogen and oxygen were fed in the same direction in order to obtain uniform current density distributions as well as reported by J. M. Sierra et. al [19]. The mass flow rates were calculated for an active area of 5 cm^2 with a stoichiometry of 1.25 and 2 for the anode and the cathode, respectively. Likewise, the concentrations of hydrogen and oxygen flows were determined, they were supplied at 1 atm of pressure and 300 K of temperature, with 25% and 25% of relative humidity for the anode and the cathode, respectively.

From these boundary conditions, the fluid dynamics equations and the electrochemical model of Ansys-Fluent®, the computational model of PEM fuel cell was solved. A segregated method, the first order scheme and SIMPLE algorithm were used to solve the equations [11].The model was evaluated in different operating potentials and thereby the current density was calculated. Using these data, polarization curves were generated to evaluate the performance of each flow field. The boundary conditions applied to the computational domain of stacks were (1) mass flow inlet, (2) pressure outlet, (3) gas diffusion layers and porous media were considered as porous jump without reactions. The flow supplied to the stacks was air.

3. Results and discussion

In this section the numerical results for different models of PEM fuel cell are presented. First, numerical results of pressure drop in stacks of 5 and 25 cm^2 are presented. These are shown by distribution contours of pressure at the interfaces: channel - gas diffusion layer (CHN / GDL) and gas diffusion layer - catalyst layer (GDL / CL), both of them at the cathode compartment. Then, numerical results of heat transfer analysis are presented by temperature contours, ohmic heating, reaction heat and enthalpy, at the cathode interface (CHN / GDL).

3.1 Pressure distributions in the stack of 5 cm^2 with single channel.

The results for serpentine design of 5 cm^2 with single channel are shown in Figure 3. In Fig. (left) it can be observed that gas pressure decreases gradually throughout the channel, from input to output channel with a maximum pressure gradient of 274 Pa. This happens due to channel length and the pressure losses generated by elbows of 90°, which are located at the end of each channel of the flow field. In Fig. (right) the maximum pressure reached was 129 Pa, which

is caused by the properties of the porous media. This pressure distribution adopted a similar pattern to the channel distribution presented previously. The average pressure at this interface was 33.7 Pa.

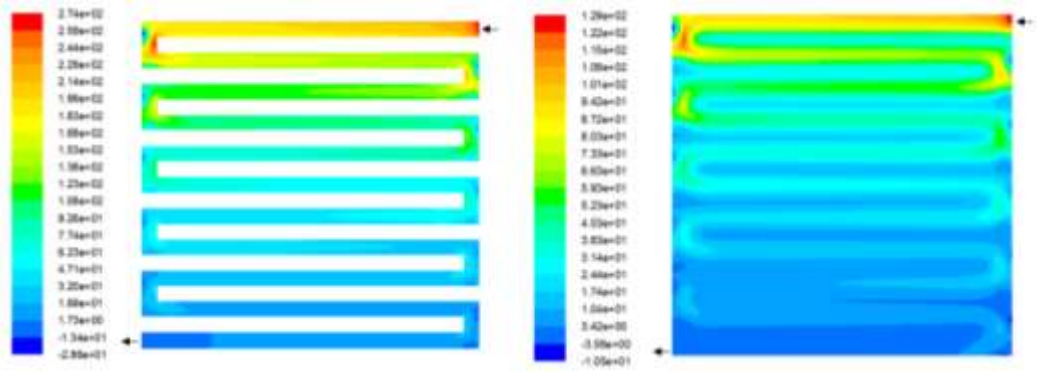

Fig. 3. Pressure distributions (Pa) for serpentine design with single channel and 5 cm^2 of active area, (left) interface (CHN/GDL) and, (right) interface (GDL/CL).

Figure 4 shows the simulation results for stacks of 2, 3 and 5 assemblies, where the gas inlet is at the top of the first assembly (right) and outlet at the bottom of the last assembly (left). For the stack with 2 assemblies, it can be observed that the pressure distribution for the first field of flow is similar to a single cell (Fig. 3a); however, for the second flow field pressure drop occurs in the region next to the gas outlet with the same magnitude as the atmospheric pressure, which affect the performance of the fuel cell. For the stack with 3 assemblies (Fig. 4b) a similar pattern distribution to the previous case is observed; however, unlike the stack with 2 assemblies, the pressure drop on the last assembly is corrected, the same goes for the stack with 5 assemblies (Fig. 4c). From these results we can deduce that flow fields with stacks of 5 cm^2 and a single channel must be at least 3 assemblies.

(a) (b) (c)

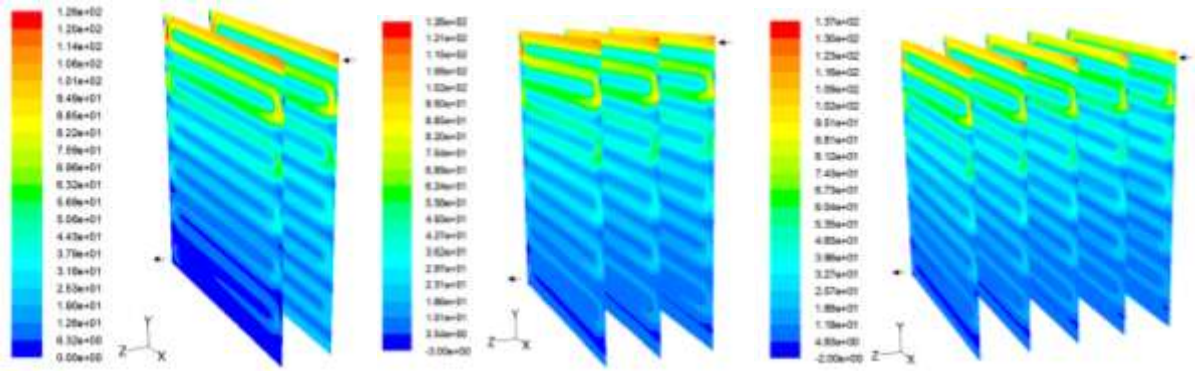

Fig. 4 Pressure distributions (Pa) in stacks with single channel configuration and active area of 5cm^2, (a) 2 assemblies, (b) 3 assemblies and, (c) 5 assemblies.

3.2 Pressure distributions in the stack of 25 cm^2 with triple channel.

The simulation results for serpentine design with three parallel channels are presented in Figure 5. Figure (left) shows that pressure distribution is significantly improved compared to the flow field with single and dual channels, this configuration provided a pressure gradient of 430 Pa, from the inlet to the outlet channels. In Figure (right) it can be observed a similar pattern of distribution, but the pressure drop was 198 Pa. This indicates that the use of parallel channels is useful for reducing pressure drop of serpentine flow fields. The average value of pressure at this interface was 19.29 Pa.

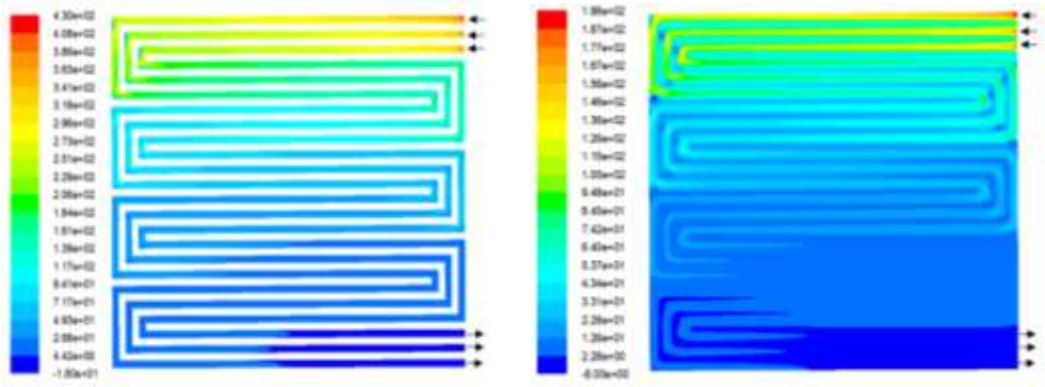

Fig. 5 Pressure distributions (Pa) for serpentine design with triple channel and 25 cm^2 of active area, (left) interface (CHN/GDL) and, (right) interface (GDL/CL).

Figure 6 shows the simulation results for stacks with 3 and 5 assemblies and three parallel channels. In Fig (left) a better pressure distribution on the three assemblies is observed, compared with two previous designs, but in the same way the first assembly has the lowest pressure values, which is not useful to use efficiently the fuel / oxidant. For the stack with 5 assemblies Fig. (right) the same distribution pattern is observed, with very low values of pressure at the first 4 assemblies.

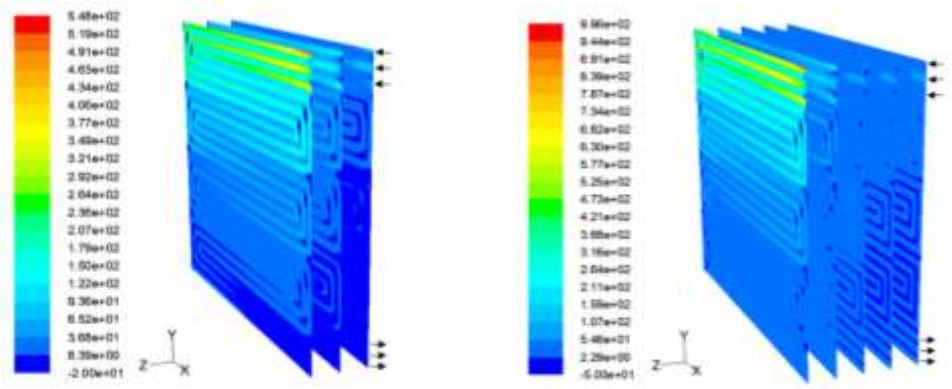

Fig. 6 Pressure distributions (Pa) in stacks with triple channel configuration and active area of 5cm^2, (left) 3 assemblies and, (right) 5 assemblies.

From this analysis it can be deduced that use of parallel channels benefits the gas distribution inside the cell, but the relationship between the width of the channel and the active area must be taken into account for the design of fuel cell stacks. Also, the location of the feed channel and its diameter must be considered, because it contributes to the first pressure drop across the stack.

3.3 Heat transfer analysis in a PEM fuel cell.

The numerical results for the fuel cell model with 5 cm^2 of active area are presented in this section. The analysis consisted on studying the temperature variation of fuel cell at different potentials operating. The analysis was done under atmospheric conditions with the aim to identify areas where there is greater heat generation in the cell. Results are presented at the GDL/CL interface for cathode side by means of temperature distributions, contours of heat reaction, ohmic heating and current density.

3.3.1 Parameters related to the heat transfer in the fuel cell.

In Fig. 7 different distribution contours for the cathode side are presented. From these results it can be seen that areas with the highest temperatures are found at the interfaces of the flow channels, where the gas reacts with the catalytic layer. Likewise, it can be seen that heat generation occurs due to processes which occur within the cell, most notably: exothermic reactions, ohmic heating, enthalpy of the reactants, the phase change of products, among others. Convection is the mechanism by which the flow dissipates more heat generated in the cell.

3.3.2 Temperature distributions in a single PEM fuel cell model.

Figure 8 shows the temperature distributions at the GDL / CL interface cathode of the fuel cell. These results were simulated at different operating voltages and under atmospheric conditions. In the figures it can be observed that as the potential of the cell is decreased the temperature increases from 300 K to 305 K. This occurs due to the generation of current in the cell and the various phenomena described above.

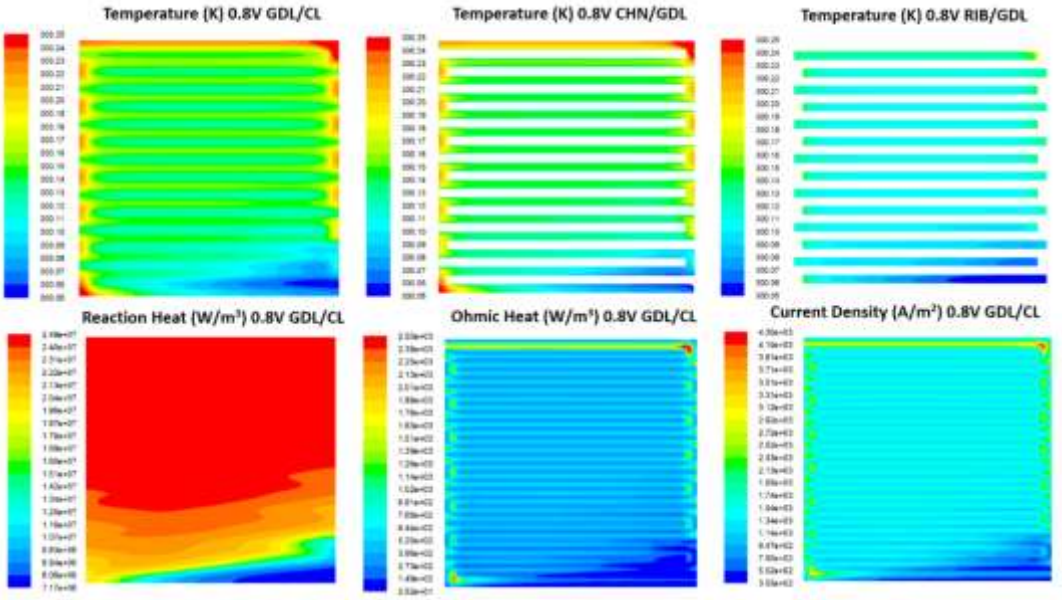

Fig. 7 Contours of distribution for different variables at the cathode compartment of the fuel cell.

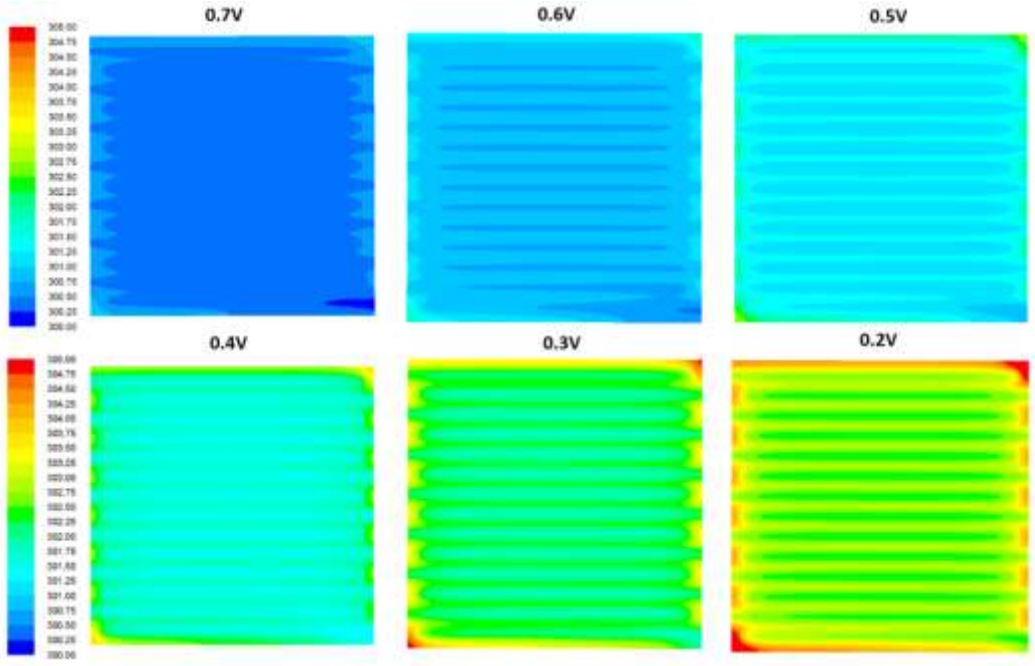

Fig. 8 Temperature distributions (K) at the cathode interface (GDL/CL) for different operating voltages.

4. Conclusions

A CFD study of flow fields in a PEM fuel cell was carried out in this work. Pressure drops that occur with serpentine designs were studied. From the numerical results, the conclusions are the following:

The pressure drops in a serpentine flow field can be reduced when the number of channels in parallel increases; this favors an even distribution of gas at GDL / CL interface, as well as the use of fuel / oxidant in the fuel cell.

The channel dimensions of 1 x 1 mm in the flow fields with 25 cm^2, are not suitable to efficiently distribute the gas on the GDL / CL interface. The channel width should be increased, otherwise the gas pressure will not be enough to cover the entire flow field due to the channel length and the elbows.

The supply system in the stacks must be modified. The design is not suitable for simultaneously supplying multiple flow fields connected in parallel form. Both the diameter, shape and location of the main supply channel should be modified to improve the gas distribution inside the fuel cell stack.

From the analysis of heat transfer could be inferred that the highest values of temperature are presented in the flow channels and the heat convection is the mechanism by which the fuel cell dissipates its heat.

Acknowledgements

The authors gratefully acknowledges to Engineering Faculty of Autonomous University of Carmen for the granted support to perform the numerical simulations in their computing equipment and the use of Ansys-Fluent® software license.

References

[1] Jeremy Rifkin, The Hydrogen Economy, Penguin Putman Inc., New York (2000).

[2] J. Larminie, A. Dicks, Fuel Cells Systems Explained, 2nd ed., Wiley, (2003).

[3] A. A. Santiago, J. Vargas, J. Cruz-Gómez, M. A. Tlenkopatchev, R. Gaviño, M. López-González, E. Riande, Synthesis and ionic transport of sulfonated ring-opened polynorbornene based copolymers. Polymer, 2011; 52: 4208-20.

[4] A. A. Santiago, J. Vargas, M. A. Tlenkopatchev, M. López-González, E. Riande, Electrochemical performance of membranes based on hydrogenated polynorbornenes functionalized with imide side groups containing sulfonated fluorinated moieties, Journal of Membrane Science 2012; 403-404: 121-8.

[5] G. Hoogers, Fuel Cell Technology Handbook, Ed. CRC Press, New York (2002).

[6] A. P. Manso, F.F. Marzo, J. Barranco, X. Garikano, M. Garmendia Mujika, Influence of geometric parameters of the flow fields on the performance of a PEM fuel cell. A review. Int. Journal of Hydrogen Energy, 2012; 37:15256-87.

[7] F. Barbir, PEM Fuel Cells – Theory and Practice, Academic Press, Elsevier, 2005.

[8] Nam Jin Hyun, Lee Kyu-Jin, Sohn Sangho, Kim Charn-Jung. Multi-pass serpentine flow-fields to enhance under-rib convection in polymer electrolyte membrane fuel cells: design and geometrical characterization. Journal of Power Sources 2009;188:14-23.

[9] Xianguo Li. Imran Sabir, Review of bipolar plates in PEMFCs: Flow-field designs. Int. Journal of Hydrogen Energy, 2005; 30: 359-71.

[10] Bladimir Ramos-Alvarado, Abel Hernandez-Guerrero, Daniel Juarez-Robles, Peiwen Li., Numerical investigation of the performance of symmetric flow distributors as flow channels for PEM fuel cells. Int. Journal of Hydrogen Energy, 2012; 37: 436-48.

[11] Fluent 6.3 – Fuel Cells Module Manual (2007).

[12] T. E. Springer, T.A. Zawodzinski, and S. Gottesfeld, Polymer Electrolyte Fuel Cell Model. J. Electrochemical Soc., 1991;138:2334-42.

[13] Jung Seok Yi, Trung Van Nguyen, Multicomponent Transport in Porous Electrodes of Proton Exchange Membrane Fuel Cells Using the Interdigitated Gas Distributors. J. Electrochemical. Society, 1999; 146: 38-45.

[14] J. H. Nam, M. Kaviany, Effective diffusivity and water-saturation distribution in single- and two-layer PEMFC diffusion medium. Int. J. Heat and Mass Transfer 2003; 46: 4595-4611.

[15] S. Shimpalee, and J.W. Van Zee, The impact of channel path length on PEMFC flow-field design. J. Power Sources, 2006; 160: 398-406.

[16] N. Djilali, and T. Berning, Computational model of a PEMFC with serpentine gas flow channels. J. Power Sources, 2004; 130: 149-157.

[17] T. Berning and N. Djilali, Three-dimensional computational analysis of transport phenomena in a PEM fuel cell, a parametric study. J. Power Sources, 2003; 124: 440-452.

[18] Um S, Wang CY. Three-dimensional analysis of transport and electrochemical reactions in polymer electrolyte fuel cells. J Power Sources 2004;125:40-51.

[19] J.M. Sierra, J. Moreira, P.J. Sebastian, Numerical analysis of the effect of different gas feeding modes in a proton exchange membrane fuel cell with serpentine flow-field. J. Power Sources, 2011; 196: 5070-5076.

[20] J. M. Sierra, P. J. Sebastian, S.A. Gamboa, Study of activation losses and ohmic resistance in a PEM fuel cell using computational fluid dynamics. ECS Transactions, 2009; 20 (1): 395-405.

[21] Fang-Bor Weng, Ay su, Guo-Bin Jung, Yen-Chiao Chiu, Shih-Hung Chan, Numerical prediction of concentration and current distributions in PEMFC. J. Power Sources, 2005; 145: 546-554.

[22] J. A. Alanís Navarro, Diseño, fabricación y caracterización de celdas de combustible de intercambio protónico utilizando tecnología MEMS, Tesis de Doctorado, Instituto de Energías Renovables, Universidad Nacional Autónoma de México (2014).